

# Synthesis of Eu-doped (Gd,Y)<sub>2</sub>O<sub>3</sub> transparent optical ceramic scintillator

Young Kwan Kim, Ho Kyung Kim,<sup>a)</sup> and Do Kyung Kim<sup>b)</sup>

*Department of Materials Science and Engineering, Korea Advanced Institute of Science and Technology (KAIST), 373-1 Kusong-dong, Yusong, Taejon 305-701, Korea*

Gyuseong Cho

*Department of Quantum and Nuclear Engineering, Korea Advanced Institute of Science and Technology (KAIST), 373-1 Kusong-dong, Yusong, Taejon 305-701, Korea*

(Received 4 June 2003; accepted 21 October 2003)

A novel process for transparent oxide ceramic scintillator with a composition of Gd<sub>1.94-x</sub>Y<sub>x</sub>Eu<sub>0.06</sub>O<sub>3</sub> was developed. The process consists of a glycine–nitrate combustion synthesis of nano-sized starting powder and subsequent controlled sintering and annealing steps. The organic molecules remaining in the as-combusted powder were efficiently removed by the combined heat-treatment at vacuum and air atmospheres. Hot-pressed ceramic scintillators show transparent optical state and high light output. Transparent optical ceramic scintillator with a high content of Gd (up to 80 mol%) was fabricated by the process. The measured light output of Gd<sub>1.54</sub>Y<sub>0.4</sub>Eu<sub>0.06</sub>O<sub>3</sub> ceramic scintillator was about two times higher than that of CdWO<sub>4</sub> single crystal.

In a typical radiation detection system, the scintillator plays the key role of converting the incident energy of ionizing radiation into scintillation light photons, then the emitted lights are collected by the under-laid photosensor. This specific application requires an ideal scintillator that has high light output, fast decay property, low afterglow, and so forth. Recently, a large number of new scintillator systems has been reviewed,<sup>1</sup> resulting, in part, with the development of a new class of scintillator: the polycrystalline ceramic scintillator.<sup>2</sup>

Discrete CdWO<sub>4</sub> single crystals are generally used in medical/industrial x-ray computed tomography (CT). Newly developed ceramic scintillators offer uniform codoping on a molecular level with special additives and a complex composition that cannot be obtained by single-crystal methods. A typical shortcoming of polycrystalline ceramic as a discrete scintillation element is its low optical transmittance due to microstructural heterogeneities, such as pores and grain-boundaries in the polycrystalline body. Light photons generated by the scintillation mechanism can be practically utilized when they successfully escape from the discrete scintillator element. Lowered optical transmittance by light scattering results

in a decreased light escape probability and, thus, finally lowers light output. Only a few kinds of ceramics, such as Gd<sub>3</sub>Ga<sub>5</sub>O<sub>12</sub>:(Cr<sup>3+</sup>,Ce),<sup>3,4</sup> Gd<sub>2</sub>O<sub>2</sub>S:(Pr,Ce,F),<sup>5,6</sup> and (Gd,Y)<sub>2</sub>O<sub>3</sub>:Eu,<sup>7</sup> have successfully been prepared as a transparent ceramic scintillator because the perfect elimination of pores is very difficult through the normal sintering step. To achieve highly transparent ceramic scintillator, it is necessary to have a specific scintillator ceramic powder that is nanocrystalline in size, of high purity, has a high specific surface area and less agglomeration, and shows full densification by the subsequent controlled sintering step.<sup>2</sup> For example, the starting powder of Gd<sub>3</sub>Ga<sub>5</sub>O<sub>12</sub>:Cr<sup>3+</sup>,Ce was prepared by the ammonium hydroxide method<sup>3,4</sup> and that of Gd<sub>2</sub>O<sub>2</sub>S:Pr,Ce,F was synthesized by the halide flux method<sup>5</sup> and the sulfite precipitation method. In cases of (Gd,Y)<sub>2</sub>O<sub>3</sub>:Eu<sup>7</sup> and Lu<sub>2</sub>O<sub>3</sub>-based<sup>8</sup> ceramic scintillators, the oxalate coprecipitation method was used to obtain a powder for the sintering of the ceramic scintillator.

The glycine–nitrate combustion method, used in this study, is an advantageous process for the synthesis of nanocrystalline powders<sup>9</sup> in many complex oxide ceramic systems, especially Y<sub>2</sub>O<sub>3</sub>-based systems,<sup>10</sup> because the glycine forms a complex salt with various metal ions. The compositional control with the combustion method is easier than with the wet chemistry method. The combustion method was recently used for Lu<sub>2</sub>O<sub>3</sub> ceramic scintillator.<sup>11</sup> The Lu<sub>2</sub>O<sub>3</sub> ceramic scintillator, however, shows a low optical transmittance. There

<sup>a)</sup>Present address: Graduate School of East-West Medical Science, Kyung Hee University, 1 Seochun, Kiheung, Yongin, 449-701, Korea.

<sup>b)</sup>Address all correspondence to this author.  
e-mail: dkkim@kaist.ac.kr

has been no report on the successful fabrication of the transparent optical ceramic scintillator with the combustion-synthesized powder.

In this study, a glycine–nitrate combustion method and the subsequent controlled sintering step were used to produce  $(\text{Gd,Y})_2\text{O}_3\cdot\text{Eu}$  ceramic scintillator, which is a promising scintillator system for the medical/industrial x-ray CT-scanner.<sup>2</sup> Previous studies about this compound showed that maximum content of  $\text{Gd}_2\text{O}_3$  was 50 mol% to obtain the optical transmittance, and the optimal composition was chosen as  $\text{Gd}_{0.60}\text{Y}_{1.34}\text{Eu}_{0.06}\text{O}_3$ .<sup>7</sup> A higher content of Gd element in the  $(\text{Gd,Y})_2\text{O}_3$  scintillator is expected to have a high scintillation intensity due to its larger x-ray stopping power. The increase of Gd content in transparent ceramic scintillator is one of the purposes of this study. The emitted scintillation light spectra were measured and compared with those of  $\text{CdWO}_4$  single-crystal scintillator.

The powder synthesis method used in this work was the glycine–nitrate combustion process.<sup>12</sup> An experimental composition was chosen as  $\text{Gd}_{1.94-x}\text{Y}_x\text{Eu}_{0.06}\text{O}_3$  ( $x = 0.0, 0.2, 0.4, 0.6, 0.97, \text{ and } 1.34$ ). The stoichiometric molar ratio of glycine/nitrate was calculated by the method of Jain et al.<sup>13</sup> and was used for the synthesis of all of the powder composition. The as-synthesized powder was ball-milled for 24 h using zirconia balls in an isopropanol liquid medium. After drying, heat-treatment was conducted for 8 h at 400 °C. Heat-treatment conditions were (i) vacuum 8 h, (ii) vacuum 4 h and air 4 h, and (iii) air 8 h. The prepared powder was sintered to transparent ceramic by the hot-pressing process at 1400 °C for 2 h with a pressure of 30 MPa in an Ar atmosphere. A post heat-treatment was conducted at 1150 °C for 2 h in air to improve the optical transparency and the light output. Crystalline structures of specimens were investigated with an x-ray diffraction (XRD) analysis. Powder morphology was examined using scanning electron microscopy (SEM) and transmission electron microscopy (TEM). The content of the organic molecule in the scintillator powder was detected by Fourier transform infrared (FTIR) spectroscopy (FTLA2000-154, ABB Inc., Quebec, Canada) and an elemental analyzer (EA; EA1110, CE Instruments, Milan, Italy).

For the excitation of the scintillator, an x-ray generator with a tungsten target was operated at 100 kVp. The emitted scintillation light spectrum as a function of wavelength was measured by the spectrometer (USB2000, Ocean Optics Inc., Dunedin, FL) incorporating the linear charge-coupled device (CCD) array as a photosensor. The relationship between the measured scintillation light spectrum emitted from the scintillator,  $S_M(\lambda)$ , and the generated scintillation light spectrum within the scintillator,  $S_0(\lambda)$  can be given by

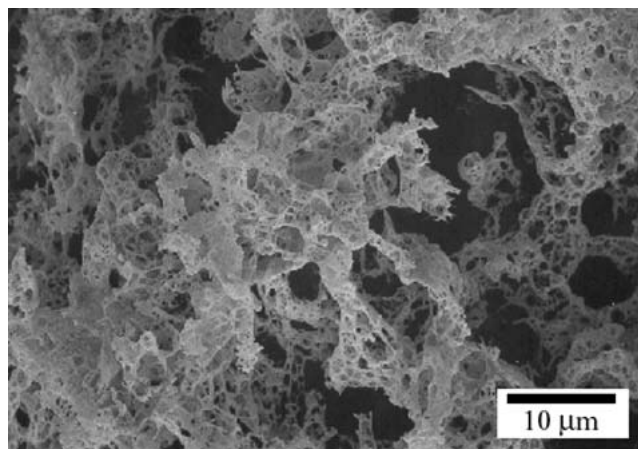
$$S_M(\lambda) = \int S_0(\lambda')\eta(\lambda,\lambda')d\lambda' \quad , \quad (1)$$

where  $\lambda$  is a wavelength and the kernel  $\eta(\lambda,\lambda)'$  is the spectral response function or simply the quantum efficiency of the spectrometer. The light output is calculated by

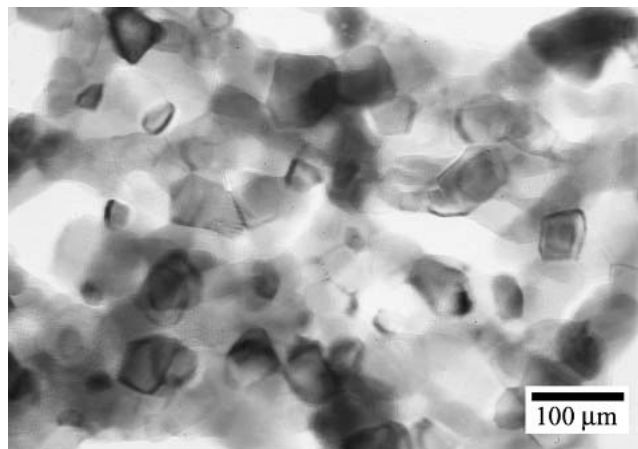
$$Y = \int S_M(\lambda)d\lambda \quad . \quad (2)$$

The correction for nonuniformity of the quantum efficiency of the spectrometer with the wavelength variation was not considered in this study. All ceramic specimens have the same thickness of 1 mm, which is much smaller than the lateral dimension. The escaped light was collected by an optical fiber with an aperture size of 1 mm in diameter.

The synthesized powder shows a single cubic phase in the XRD result. Gadolinium and yttrium oxides form the complete solid solution. The as-synthesized powder has a foamy and porous structure, as shown in Fig. 1(a), which



(a)



(b)

FIG. 1. Electron micrographs of the synthesized  $(\text{Gd,Y})_2\text{O}_3$  ceramic powder. (a) SEM micrograph shows a foamy shape in as-combusted state, and (b) TEM micrograph shows a nano-sized primary particle of powder. Primary particle size was 58 nm from the measurement from TEM micrographs.

is a typical microstructure of powders prepared by the glycine–nitrate combustion process. The TEM micrograph, shown in Fig. 1(b), shows the shape and size of primary particles. Equiaxed and nanometer-sized primary particles are essential for the full densification of ceramics. The measurement of TEM images showed the mean size of primary particles to be 58 nm. Due to the light agglomeration of the as-synthesized powder, ball-milling was enough to get the submicrometer secondary particles, which is necessary to improve the forming ability of powder.

The as-synthesized powders produced by the combustion method commonly contain some carbon and nitrogen ligands that are caused by incomplete reaction at the combustion process. For the full densification of ceramics, organic molecules need to be removed from the powder because the organic molecules leave the trapped gas molecule which is one of major reasons for residual pores.<sup>2</sup> Temperatures of the powder heat-treatment must be carefully determined because nanocrystalline powders synthesized by the combustion method show an exaggerated particle growth when subjected to a high-temperature heat treatment.<sup>9</sup> Based on the report that  $Gd_2O_3$  powder synthesized by the combustion method maintains the initial particle size and shape at 300–500 °C,<sup>14</sup> 400 °C was selected as the heat-treatment temperature of the powder.

Figure 2 shows the results of the FTIR analysis. At a wavenumber of 3446.5  $cm^{-1}$ , a broad peak was detected that was caused by the –OH ligand. A peak of 1635.5 was also caused by –OH. Other peaks were identified as: 1384.7  $NO_3^-$ ; 1417.6 C–O; 1508.2, 1521.7, and 1541.0  $-NH_2$ .<sup>15–20</sup> Amounts of these organic molecules

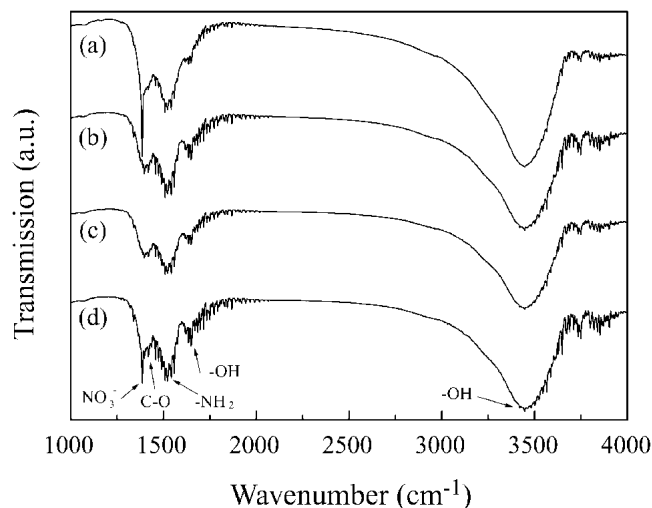


FIG. 2. FTIR results of  $Gd_{0.60}Y_{1.34}Eu_{0.06}O_3$  powders after each heat-treatment step. A plot of the as-synthesized powder (a) was compared with those of heat-treated powders. Heat-treatment conditions were (b) vacuum 8 h, (c) vacuum 4 h and air 4 h, and (d) air 8 h at 400 °C.

were decreased after the powder heat-treatment. But, the heat-treatment at air atmosphere was not sufficient to remove  $NO_3^-$  ligand. A sharp  $NO_3^-$  peak at 1384.7  $cm^{-1}$  was observed even after the heat treatment in the air atmosphere. As shown in Table I, the elemental analysis reveals more quantitative results. Air heat-treatment removed the carbon and hydrogen most efficiently, and vacuum heat-treatment was efficient for the removal of nitrogen. Because most of the carbon molecules exist as C–O bond, oxygen is needed to transform C–O ligand into carbon dioxide. Nitrogen exists in the form of  $-NH_2$  or  $NO_3^-$  and is transformed into  $N_2$ , NO, or  $NO_2$  during vacuum heat-treatment. Therefore, it is concluded that the combined heat-treatment in vacuum and air atmosphere is most efficient at removing the organic molecules.

Figure 3 shows a macroscopic view of  $Gd_{0.60}Y_{1.34}Eu_{0.06}O_3$  transparent ceramic scintillator. The thickness of the specimen is 1 mm and the diameter is 18 mm. In the composition range from  $Gd_{1.54}Y_{0.40}Eu_{0.06}O_3$  to  $Gd_{0.60}Y_{1.34}Eu_{0.06}O_3$ , (up to 80 mol% of Gd), the ceramic scintillators give a transparent optical state. In Fig. 4, the measured light spectra of  $Gd_{1.94}Eu_{0.06}O_3$ ,  $Gd_{1.54}Y_{0.40}Eu_{0.06}O_3$ , and  $Gd_{0.60}Y_{1.34}Eu_{0.06}O_3$  ceramic scintillators are compared with that of  $CdWO_4$  single crystal. Transparent ceramic scintillators show higher scintillation intensity. At higher compositions of  $Gd_2O_3$ , such as  $Gd_{1.94}Eu_{0.06}O_3$  and  $Gd_{1.74}Y_{0.20}Eu_{0.06}O_3$ , the phase of scintillators was changed from cubic to monoclinic. The sintered ceramic scintillators of these compositions show optically opaque states and low scintillation intensity. From Fig. 4 and Eq. (2), the transparent  $Gd_{1.54}Y_{0.40}Eu_{0.06}O_3$  ceramic scintillator shows about two times higher light output than that of  $CdWO_4$  single crystal.

In conclusion, the glycine–nitrate combustion process was used to synthesize nano-sized starting powder for the Eu-doped  $(Gd,Y)_2O_3$  ceramic scintillator. The synthesized powder shows the single cubic phase, and gadolinium and yttrium oxides form the complete solid solution. As-synthesized powder has a foamy agglomerated structure; the equiaxed nanometer-sized primary particles were lightly agglomerated to form porous secondary particles. The organic molecules remaining in the as-synthesized powder were efficiently removed by the combined heat-treatment at vacuum and air atmospheres.

TABLE I. Elemental analysis result of  $Gd_{0.60}Y_{1.34}Eu_{0.06}O_3$  powders after heat-treatment step. Heat treatment was conducted at 400 °C.

Element (wt%)	As-synthesized	In vacuum		
		In vacuum (8 h)	(4 h) + in air (4 h)	In air (8 h)
N	0.122 ± 0.004	0.097 ± 0.004	0.094 ± 0.002	0.113 ± 0.006
C	0.663 ± 0.014	0.299 ± 0.002	0.210 ± 0.01	0.187 ± 0.016
H	0.276 ± 0.016	0.192 ± 0.003	0.180 ± 0.004	0.184 ± 0.004

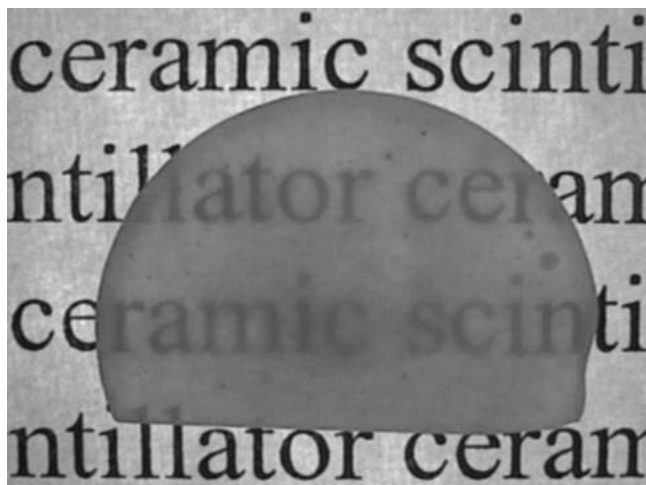


FIG. 3. Macroscopic view of the transparent  $\text{Gd}_{0.60}\text{Y}_{1.34}\text{Eu}_{0.06}\text{O}_3$  ceramic scintillator. Thickness of specimen is 1 mm.

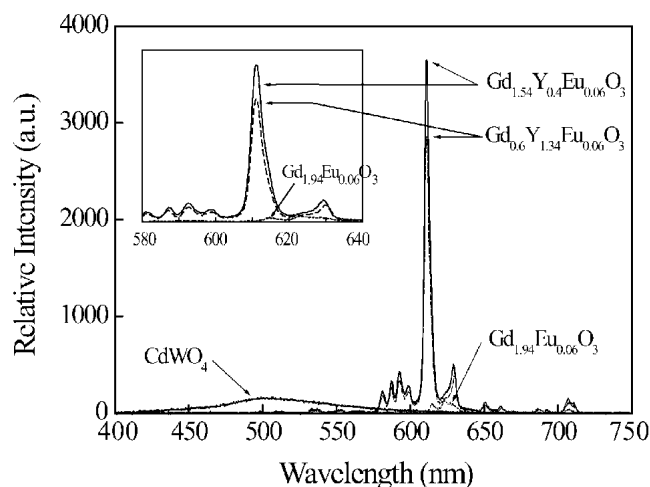


FIG. 4. Emitted scintillation light spectra of Eu-doped  $(\text{Gd,Y})_2\text{O}_3$  ceramic scintillators and  $\text{CdWO}_3$  single-crystal scintillator. Thickness of specimen is 1 mm. Selected compositions are  $\text{Gd}_{1.94}\text{Eu}_{0.06}\text{O}_3$ ,  $\text{Gd}_{1.54}\text{Y}_{0.4}\text{Eu}_{0.06}\text{O}_3$ , and  $\text{Gd}_{0.60}\text{Y}_{1.34}\text{Eu}_{0.06}\text{O}_3$ . Inset shows the detail light output spectra of transparent optical ceramic scintillators.

Hot-pressed ceramic scintillators show transparent optical state and high light output. Transparent optical ceramic scintillators with a high content of Gd (up to 80 mol%) could be fabricated by the process. The measured

light output of the  $\text{Gd}_{1.54}\text{Y}_{0.4}\text{Eu}_{0.06}\text{O}_3$  ceramic scintillator was about two times higher than that of  $\text{CdWO}_4$  single crystal.

#### ACKNOWLEDGMENT

This work was supported by the KISPEP (Korea Institute of S&T Evaluation and Planning) under Grant No. M2-0335-01-0003.

#### REFERENCES

1. W.W. Moses, Nucl. Instrum. Methods A **487**, 123 (2002).
2. C.D. Greskovich and S. Duclos, Ann. Rev. Mater. Sci. **27**, 69 (1997).
3. V.G. Tsoukala and C.D. Greskovich, U.S. Patent No. 5 318 722 (June 7, 1994).
4. G. Blasse, B.C. Grabmaier, and M. Ostertag, J. Alloy. Compd. **200**, 17 (1993).
5. H. Yamada, A. Suzuki, Y. Uchida, M. Yoshida, and H. Yamamoto, J. Electrochem. Soc. **136**, 2713 (1989).
6. J. Leppert and W. Rossner, U.S. Patent No. 5 296 163 (March 22, 1994).
7. C.D. Greskovich, D.A. Cusano, and F.A. DiBianea, U.S. Patent No. 4 466 930 (August 21, 1984).
8. A. Lempicki, C. Brecher, P. Szupryczynski, H. Lingertat, V.V. Nagarkar, S.V. Tipnis, and S.R. Miller, Nucl. Instrum. Methods A **488**, 579 (2002).
9. S. Bhaduri and S.B. Bhaduri, Nanostructured Mater. **11**, 469 (1999).
10. W.-J. Kim, J.Y. Park, S.J. Oh, Y.S. Kim, G.-W. Hong, and I.-H. Kuk, J. Mater. Sci. Lett. **18**, 411 (1999).
11. E. Zych, D. Hreniak, and W. Strek, J. Alloy. Compd. **341**, 385 (2002).
12. L.A. Chick, L.R. Pederson, G.D. Maupin, J.L. Bates, L.E. Thomas, and G.J. Exarhos, Mater. Lett. **10**, 6 (1990).
13. S.R. Jain and K.C. Adiga, Combustion and Flame **40**, 71 (1981).
14. L. Sun, J. Yao, C. Liu, C. Liao, and C. Yan, J. Lumin. **87-89**, 447 (2000).
15. N.L. Alpert, W.E. Keiser, and H.A. Szymanski, *IR Theory and Practice of Infrared Spectroscopy* (Plenum Press, New York, 1970).
16. K. Nakamoto, *Infrared and Raman Spectra of Inorganic and Coordination Compounds* (Wiley-Interscience, New York, 1978).
17. J. Baran, A.J. Barnes, and H. Ratajczak, Spectrochim. Acta. A **51**, 197 (1995).
18. T. Ye, Z. Guiwen, Z. Weiping, and X. Shangda, Mater. Res. Bull. **32**, 501 (1997).
19. M. Devereux, M. Jackman, M. McCann, and M. Casey, Polyhedron **17**, 153 (1998).
20. L. Kovacs, S. Erdei, and R. Capelletti, Solid State Commun. **111**, 95 (1999).